metals

MDPI

Article

Effect of the Hot Deformation Conditions on Structure and Mechanical Properties of AlCr/AlCrSi Powder Composites

Elena N. Korosteleva *, Gennady A. Pribytkov and Victoria V. Korzhova

Institute of Strength Physics and Materials Science of the Siberian Branch of the Russian Academy of Sciences, 2/4, pr. Akademicheskii, 634055 Tomsk, Russia; gapribyt@mail.ru (G.A.P.); vicvic5@mail.ru (V.V.K.)
* Correspondence: elenak@ispms.tsc.ru; Tel.: +7-903-913-8002

Abstract: Aluminum matrix composites usually contain strengthening particles of refractory compounds (SiC, Al_2O_3) that do not react with the Al matrix. There is a problem in producing the Al matrix composite with inclusion of metals that can generate intermetallic compounds with aluminum. In this case, a conventional sintering of powder mixtures results in high porosity due to volume growth. That is why some new methods of producing dense Al matrix composites are required. A possibility to create a dense powder Al-based composite containing hard components, such as chromium and silicon, without using the sintering process, is considered. This paper presents study results of structural and mechanical properties of Al-Cr and Al-Cr-Si composites produced by hot compaction of powder mixtures. An analysis of the relationship between mechanical properties and structures of Al-Cr and Al-Cr-Si composites is carried out. Optimal values for thermomechanical processing modes that ensure sufficient strength and plasticity are determined. It is shown that strong bonding of the aluminum particles occurs under hot deformation, and an aluminum matrix is formed that provides acceptable composite bending strength as a result. The presence of chromium and silicon hard inclusions is not a significant obstacle for aluminum plastic flow. Al-Cr and Al-Cr-Si composites produced by hot deformation of the powder mixtures can be used as cathode material for the deposition of wear-resistant nitride coatings on metalworking tools.

Keywords: Al matrix composites; powder materials; hot compaction; structure; high temperature deformation; mechanical properties

Citation: Korosteleva, E.N.; Pribytkov, G.A.; Korzhova, V.V. Effect of the Hot Deformation Conditions on Structure and Mechanical Properties of AlCr/AlCrSi Powder Composites. *Metals* **2021**, *11*, 1853. https://doi.org/10.3390/met11111853

Academic Editor: Robert Bidulský

Received: 21 October 2021
Accepted: 15 November 2021
Published: 18 November 2021

1. Introduction

Composite powder materials attract great interest due to their unique properties resulting from the synergistic effect of combining properties of structural elements. These properties make it possible to use composite materials in different areas of industry: as finished products, structural elements and tools, as well as auxiliary units in various technological processes in the field of electro-physics and chemistry. Aluminum-based metal matrix composites are an attractive group of materials due to their unique combination of properties that include low weight, acceptable strength, wear and corrosion resistance, and good ductility [1–7]. As a rule, the main studies of aluminum matrix composites concern the improvement of their functional properties [3–5,7]. The study of aluminum matrix composites with hard inclusions is of particular interest, since the production of such composites is associated with numerous problems [8,9]. In addition to analyzing the hard component's role in improving physical and mechanical properties, the problems of technological process optimization for these composites' production are also studied [10,11]. In some cases, the requirements for composites' mechanical properties are not as high as for highly loaded structural materials. Sometimes, an acceptable level of mechanical properties is one that is sufficient to ensure the functioning of the aluminum composite as part of a specific unit. In particular, it is convenient to consider composite materials as sources of multicomponent ion plasma (cathodes) for the PVD coatings formation. For example, multicomponent aluminum and chromium nitride coatings are considered as some of the

most promising coatings for cutting tools due to their high thermal stability and oxidation resistance at high temperatures (800–1000 °C) [12–15]. It was found that the coatings had the best performance characteristics at the Al:Cr = 70:30 and Al:Cr:Si = 65:25:10 (in %) element ratio [16,17]. A multicomponent plasma can be obtained by using several versions of source sets: traditional multi-cathode units, single cast cathodes or multicomponent powder cathodes. Regarding monolithic cathodes, the problem exists for Al-Cr and Al-Cr-Si alloys due to the brittle intermetallic formation obstructing material workability [18]. Powder technology is a suitable method of producing multicomponent cathodes based on Al-Cr and Al-Cr-Si, but a simple sintering mode is not convenient because of uncontrolled volume effects with a large increase in the porosity of aluminum powder alloys [19]. Hot consolidation of powder mixtures containing aluminum at temperatures below the beginning of active diffusion interaction of aluminum and chromium is one more promising method for the production of powder cathode material [20]. Such diffusion interaction leads to the brittle intermetallic compound's formation. Since the main function of the cathode is to be a source of various elements in the multicomponent plasma, the presence of intermetallic compounds in the cathode material is a rather negative factor that can affect the functional properties of the cathode material.

Intense hot deformation can cause "welding" of the adjacent aluminum particles due to the destruction of oxide films on their surface, which provides higher strength of the powder material [21–23]. Therefore, it can be expected that the high aluminum plasticity at elevated temperatures will make it possible to obtain porosity close to zero under conditions of uniaxial pressing of powder mixtures containing aluminum with brittle chromium and silicon. Taking into account a relatively low level of requirements of the strength and plasticity of cathode materials, hot compaction of aluminum base powder mixes can be a convenient method of composite cathode production. In addition to cathode materials, the hot compacting technology can be applied to the production of other materials with a medium degree of strength using a ductile aluminum matrix with hard inclusions.

Unfortunately, a number of problems related to the influence of thermomechanical impact on the structure formation of powder compacts and their mechanical properties are still poorly investigated. In this regard, the study of the relationship between the modes of thermomechanical treatment, the formed structure of Al-Cr and Al-Cr-Si powder composites, and their mechanical properties, is relevant. The attention is focused on the possibility of obtaining a non-porous aluminum matrix composite with chromium and silicon inclusions without using the sintering process. Study results can clarify whether it is possible to produce Al-based composite materials with hard particle inclusions by hot-compacting powder mixtures.

This paper presents the results of the study of structure, mechanical properties and fracture characteristics of composites produced by hot compaction of powder mixtures of Al-Cr and Al-Cr-Si compositions, when the temperature and hot deformation degree of compacts are varied. The experimental results make it possible to optimize the modes of hot-compacting Al-Cr and Al-Cr-Si powder mixtures to produce dense and sufficiently strong cathodes for vacuum arc evaporation and magnetron sputtering of wear-resistant coatings.

2. Materials and Methods

Pure element powders of aluminum (<100 μm, RUSAL Co., Russia), chromium (<50 μm, POLEMA Co., Russia), and silicon (<50 μm, RUSAL Co., Russia) were used to prepare Al-Cr and Al-Cr-Si powder mixtures. For the two-component mixture, a 70Al + 30Cr (in %) element ratio was used. In the second variant, the silicon was added in the mixture at the component ratio of 65Al + 25Cr + 10Si (in %). Powder morphology is shown in Figure 1. The particles of aluminum powder produced by melt spraying are crystallized rounded droplets of various sizes. The shape of the particles is nearly spherical and elongated. Chromium powder particles are crystalline agglomerates in a faceted crystal form of various shapes and sizes. Silicon powder has a shard shape. In accordance with the

physicochemical characteristics, these powder components occupied the corresponding volume fraction in the mixture (Table 1).

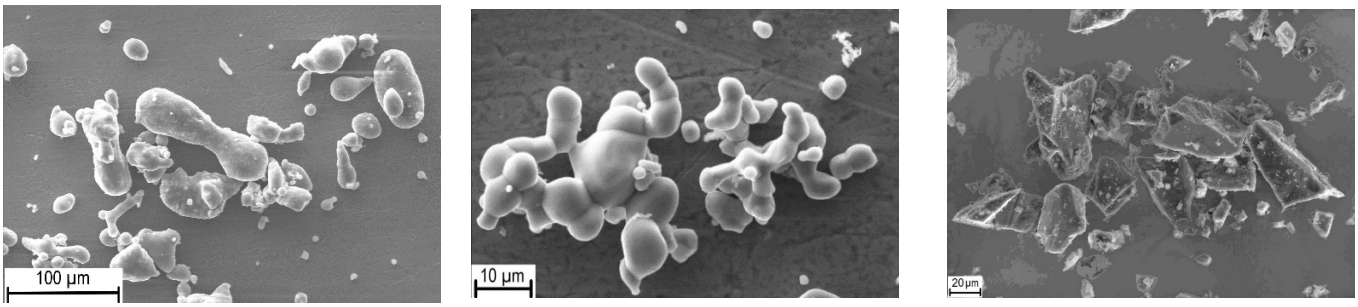

(**a**) (**b**) (**c**)

Figure 1. Typical view of the powders: (**a**) Al; (**b**) Cr; (**c**) Si.

Table 1. Volume fraction of powder components in the mixtures, %.

Mixture Composition	Components (vol/%)		
	Al	Cr	Si
$Al_{70}Cr_{30}$	76.4	23.6	-
$Al_{65}C_{25}rSi_{10}$	68.4	19.0	12.6

Cold-compacted preforms were obtained by the bilateral compression of powder mixtures in cylindrical molds of various diameters, from 20 to 39 mm. Subsequent preform heating was carried out in the range of 350–550 °C. After heating to the desired temperature, the preforms were compacted in a larger diameter (40 mm) mold. The scheme of the two-stage compaction is shown in Figure 2.

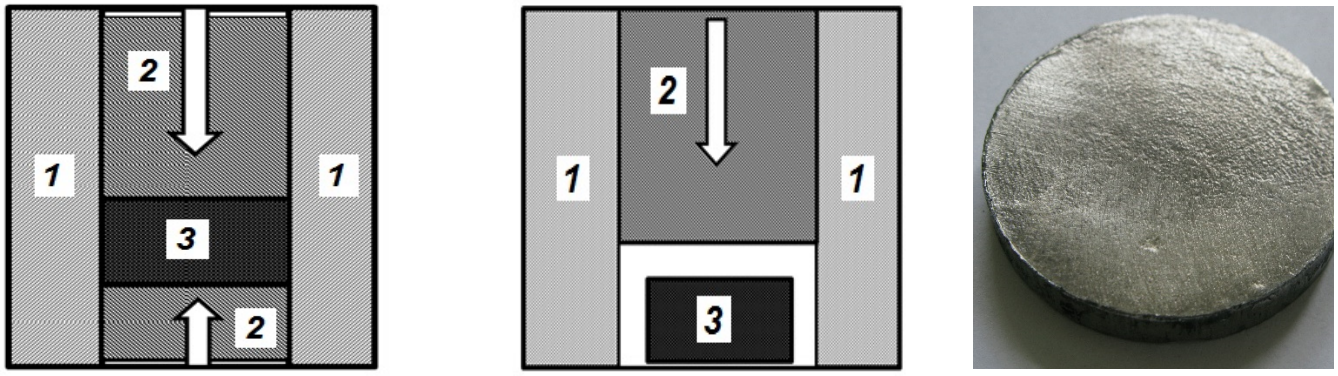

(**a**) (**b**) (**c**)

Figure 2. Scheme of the two-stage compaction; *1*—mold matrix; 2—upper and bottom punch; *3*—specimen; (**a**) cold-pressing of the powder mixture in press molds with diameters of 20–39 mm; (**b**) compression of heated preform in a press mold with diameter of 40 mm; (**c**) hot-compacted specimen with diameter of 35 mm.

The degree of deformation ε_h during hot compaction was calculated by Formula (1), using the height of cylindrical samples before (H_0) and after (H_1) hot compaction:

$$\varepsilon_h = \left(1 - \frac{H_1}{H_0}\right) \times 100\%, \quad (1)$$

The initial and final porosities θ were calculated from the results of volume measurements and weighing powder compacts using Formula (2):

$$\theta = \left(1 - \frac{\rho_R}{\rho_{Th}}\right) \times 100\%, \quad (2)$$

where ρ_{Th} is the theoretical density of material calculated from Al, Cr, and Si densities, and ρ_R is the actual density.

Three-point bend tests of rectangular parallelepiped shape specimens (height of 5 mm, width of 5 mm, and length of 30 mm) cut off from hot-pressed powder composites were carried out on an INSTRON 5582 universal test machine (INSTRON, Norwood, MA, USA) at a loading rate of 0.5 mm/min. Bend strength was calculated using Formula (3):

$$\sigma_B = \frac{3P_{max}\mathrm{L}}{2a^2b}, \quad (3)$$

where P_{max} is the maximum load on the ($P-\Delta h$) curve; L is the distance between support roller axles (25 mm); a is the sample height; and b is the sample width. The plasticity of the sample material was calculated as the ratio of deformation value before fracture Δh_{pl} to the length L of the sample working part. The hot-compacted powder material structure was investigated through optical metallography (AXIOVERT-200MAT, Zeiss, Germany), X-ray diffraction (DRON-7 diffractometer, Burevestnik, Russia) in CoKα-radiation, and scanning electron microscopy (SEM) with energy-dispersive X-ray microanalysis (EDX) (LEO EVO 50, Zeiss, Germany).

3. Results and Discussion

A typical view of the microstructure of powder compositions subjected to hot compaction is shown in Figure 3. After hot compaction, at the maximum temperature of 550 °C, the composite microstructure is a continuous aluminum matrix with inclusions of chromium particles (Figure 3a) or chromium and silicon particles (Figure 3b). There are a few pores concentrated mainly near the "inclusion–aluminum" interface. No other phase inclusions were found in the metallographic study [20]. According to X-ray diffraction patterns (Figure 3 c,d), only the Al, Cr, and Si reflections were present.

It is known that the equilibrium solubility of chromium in solid aluminum at 600 °C is 0.25 at.%. Silicon atoms can be dissolved by up to 1.5 at.% at 577 °C [24,25]. Under high temperatures of heating and subsequent deformation, the Al-Cr and Al-Si solid solution formation occurs, which influences line shift in the X-ray diffraction patterns (Figure 3c,d). The calculation of the micro-distortion of the lattice parameters in the X-ray analysis of hot-pressed compacts showed a slight decrease in the lattice parameter of the aluminum matrix. It may be a confirmation of the boundary interaction of chromium and silicon with aluminum particles. In addition, a highly defective structure of the compact aluminum matrix is formed as a result of thermomechanical processing, which can stimulate surface diffusion of atoms [26]. Since the hot deformation process takes place over a short time interval (20–30 min), the mass transfer is insufficient for forming a noticeable volume of solid solution phase during this period.

In a study of any powder material, qualitative and quantitative characteristics of residual porosity play an important role, as well as porosity evolution under external impact conditions [27]. From the point of view of mechanical properties of aluminum matrix composites, the minimum pore volume content with finely dispersed rounded morphology is preferable. As it is well known [28], it is almost impossible to achieve a completely non-porous structure during cold-pressing. The limiting value of green compact residual porosity can vary from 4–8% to 20–30%, depending on a powder's hardness and plasticity. Therefore, in the study of aluminum matrix composite, it was important to evaluate the formed porosity and its changes in the hot compaction process. Since aluminum is a highly ductile metal, the aluminum base powder mixture is easily pressed at room temperature to almost 95% of the theoretical density (up to 5% porosity).

The use of hard chromium particles as an additive, and then the addition of silicon in the mixtures, complicates the cold-compacting of the billets, but still allows us to achieve a 10% porosity.

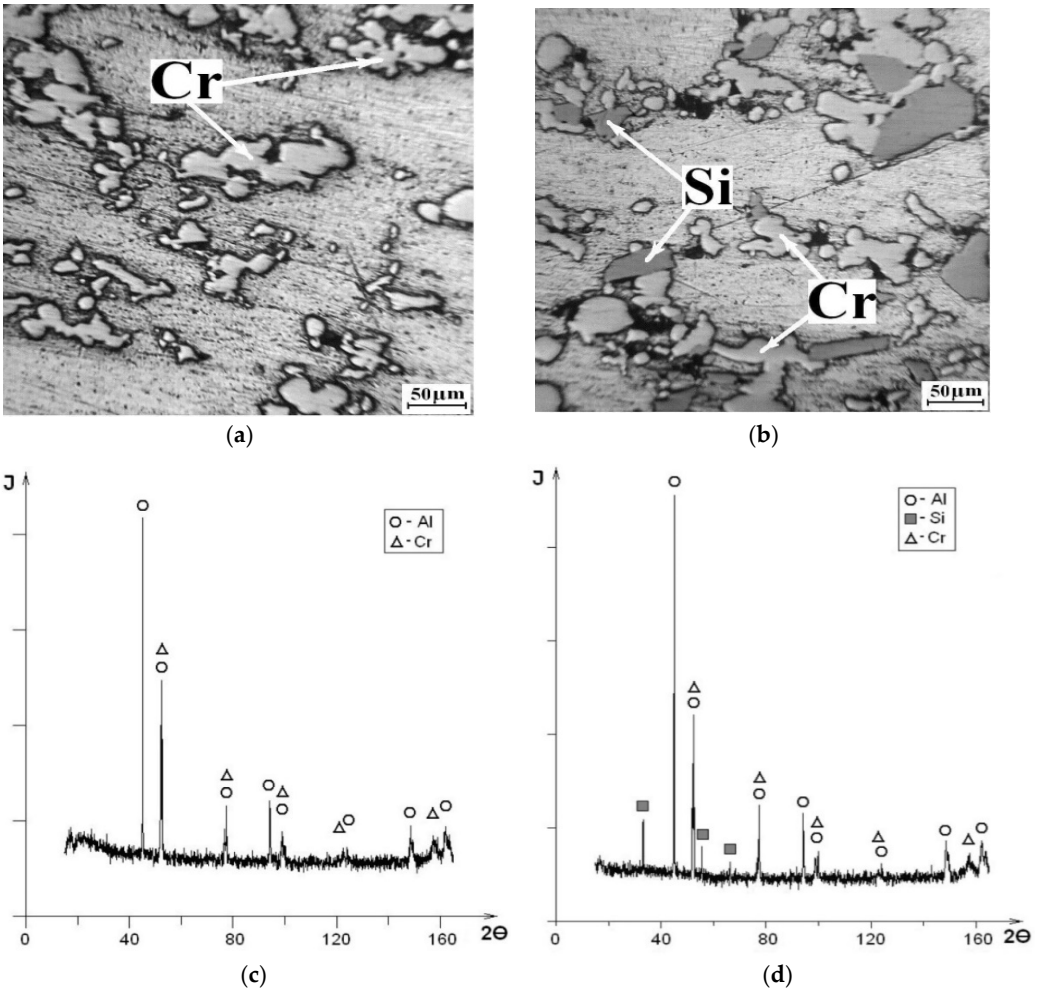

Figure 3. Optical metallography image and XRD patterns of powder composites hot-compacted at 550 °C by 0.5 GPa pressure: (**a**,**c**) $Al_{70}Cr_{30}$; (**b**,**d**) $Al_{65}Cr_{25}Si_{10}$.

The porosity of compacts after hot compaction of cold-pressed billets was varied in the range of 2.5–7.5%, depending on the powder mixture composition, temperature, and deformation degree during compaction (Figure 4). Minimum porosity (about 3.5%) was obtained with aluminum–chromium compositions. $Al_{65}Cr_{25}Si_{10}$ composite porosity significantly decreased with temperature gain of the hot compaction: 7.5% at 350 °C, 6.0% at 450 °C, and 4.8% at 550 °C. The porosity of the hot-compacted $Al_{65}Cr_{25}Si_{10}$ composition specimens was on average 2% higher than that for the $Al_{70}Cr_{30}$ composition specimens at the same pressures. Under a high degree of deformation, the matrix integrity is destroyed. Additional defects (pores and microcracks) are formed at the boundary of the aluminum matrix with inclusions. Therefore, a certain porosity increase is observed with the increase in the degree of deformation (Figure 4).

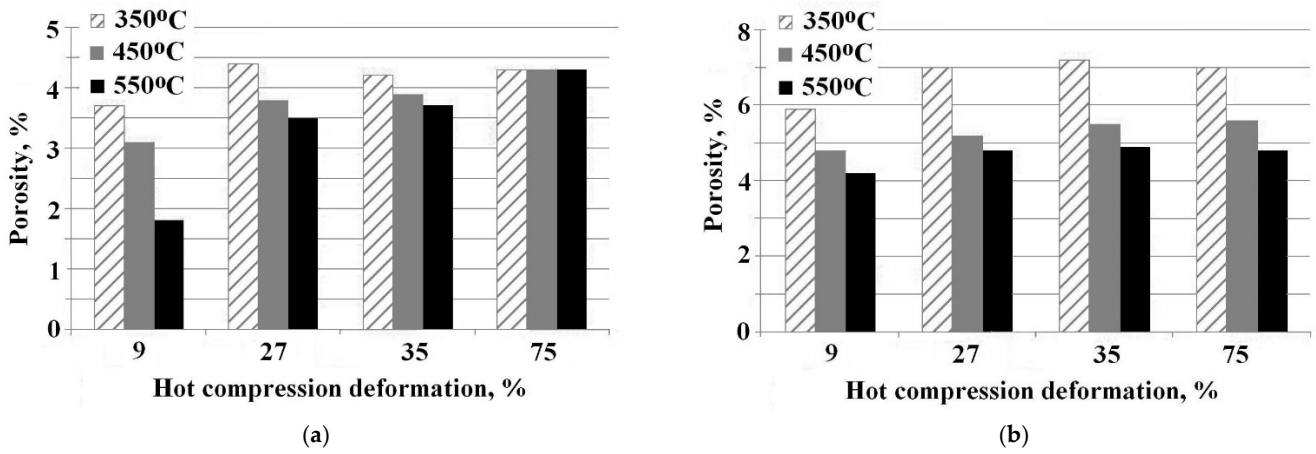

Figure 4. Porosity changes of $Al_{70}Cr_{30}$ (**a**) and $Al_{65}Cr_{25}Si_{10}$ (**b**) composites during the hot compaction process with different processing conditions.

The effect of the hot compaction conditions on the strength and plasticity under three-point bending tests at different temperatures is shown in Figures 5 and 6.

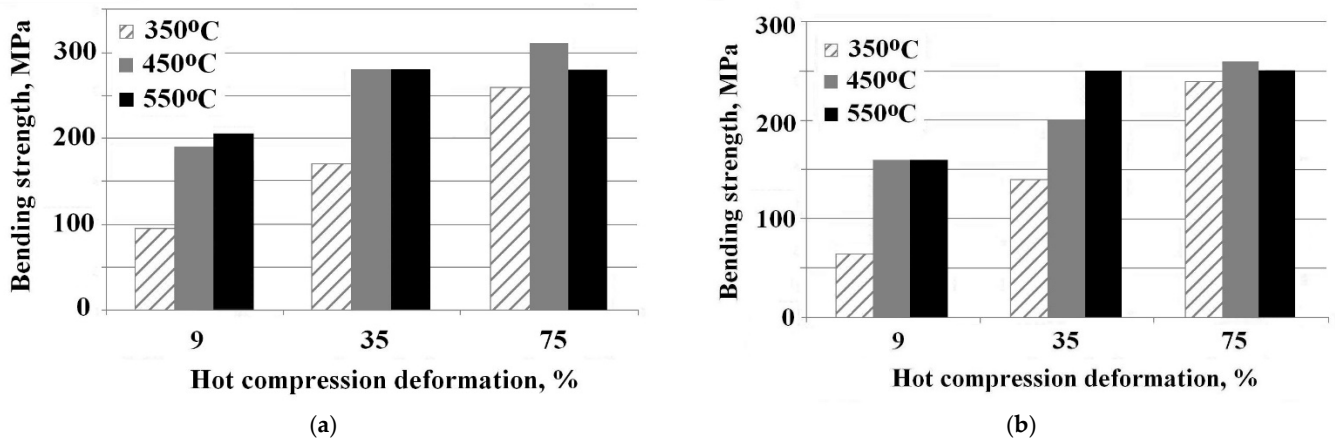

Figure 5. Relation between bending strength and hot compression deformation of $Al_{70}Cr_{30}$ (**a**) and $Al_{65}Cr_{25}Si_{10}$ (**b**) powder composites compacted at different temperatures.

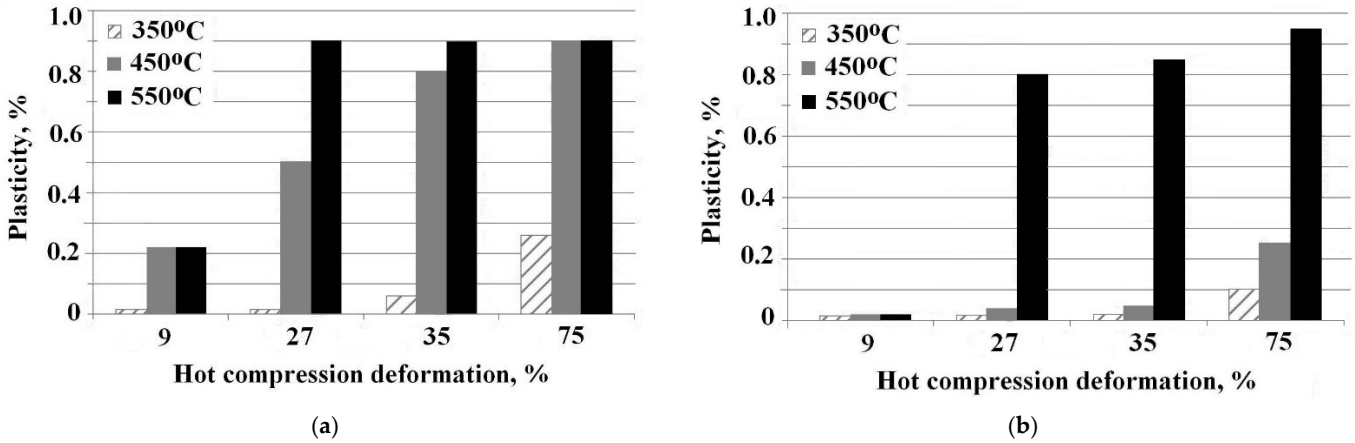

Figure 6. Relation between plasticity at the bending tests and hot compression deformation of $Al_{70}Cr_{30}$ (**a**) and $Al_{65}Cr_{25}Si_{10}$ (**b**) powder composites compacted at different temperatures.

These results show that there are certain value limits on the temperature and deformation degree to achieve high strength and high plasticity. For the $Al_{70}Cr_{30}$ composite, these ε_h limits are 35% at 450 °C and 27% at 550 °C, respectively. For the $Al_{65}Cr_{25}Si_{10}$ composite, the value limit ε_h is 27% at 550 °C, while at lower temperatures, the strength and plasticity increase monotonically with increasing deformation degree ε_h in a range from 9 to 75%. The character of dependencies is consistent with the conventional concept of powder material consolidation by thermo-force processing [29]. The higher the temperature and deformation degree, the more intense the process of adjacent particles' "welding", and the higher the physical–mechanical properties. Thus, the strength of composites increases (Figure 5) despite the increase in porosity under a growth of the deformation degree (Figure 4).

The microhardness behavior of the aluminum matrix in hot-compacted powder compositions after hot pressing has the opposite tendency (Figure 7). Porosity's influence on hardness turned out to be weaker than that on the bending strength. With the increase in treatment temperature and deformation degree, the microhardness increase occurs. The addition of silicon results in further microhardness increase in the aluminum matrix after high temperature deformation. In this case, a possible reason for microhardness increase is the hardening effect due to chromium and silicon atoms' diffusion into aluminum. Accelerated diffusion in the defective structure that forms during a large deformation gives a noticeable volume fraction of the solid solution that may be confirmed by the XRD line shift (Figure 3c,d).

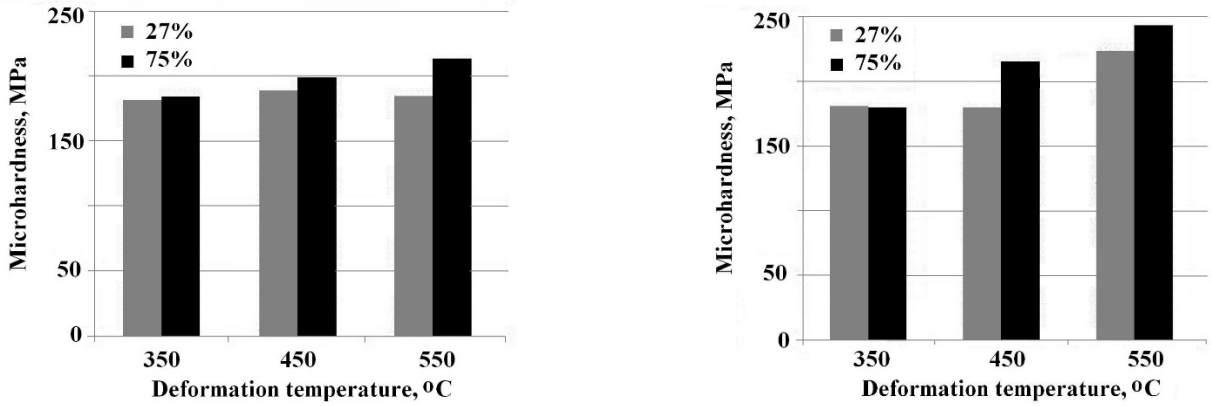

Figure 7. Effect of the hot deformation temperature on aluminum matrix microhardness of $Al_{70}Cr_{30}$ (**a**) and $Al_{65}Cr_{25}Si_{10}$ (**b**) powder composites.

The results of fracture surface study of hot-deformed powder composite specimens broken down during bending tests are presented below. Features of composite fracture surfaces obtained by varying the temperature and deformation degree during hot compaction were studied to clarify the effect of temperature and hot deformation on the "welding" of powder particles of different elements.

Figures 8a and 9a show that $Al_{70}Cr_{30}$ and $Al_{65}Cr_{25}Si_{10}$ powder billets keep the intraparticle morphology of green preforms at low temperatures and low deformation degrees. In the case of $Al_{70}Cr_{30}$ composites, strong interparticle bonds are absent, and the strength and plasticity of the composite nearly correspond to that of cold-compacted preforms. During intensive thermomechanical processing (T = 550 °C, ε = 75%), a continuous aluminum matrix is formed with inclusions of chromium particles. Ductile fracture features in aluminum matrix areas, combined with protruding chromium particles, can be seen on the fracture surface image (Figure 8d). It can be seen that adjacent aluminum particles are welded, and chromium particles remain non-deformed; the element distribution confirms this (Figure 8).

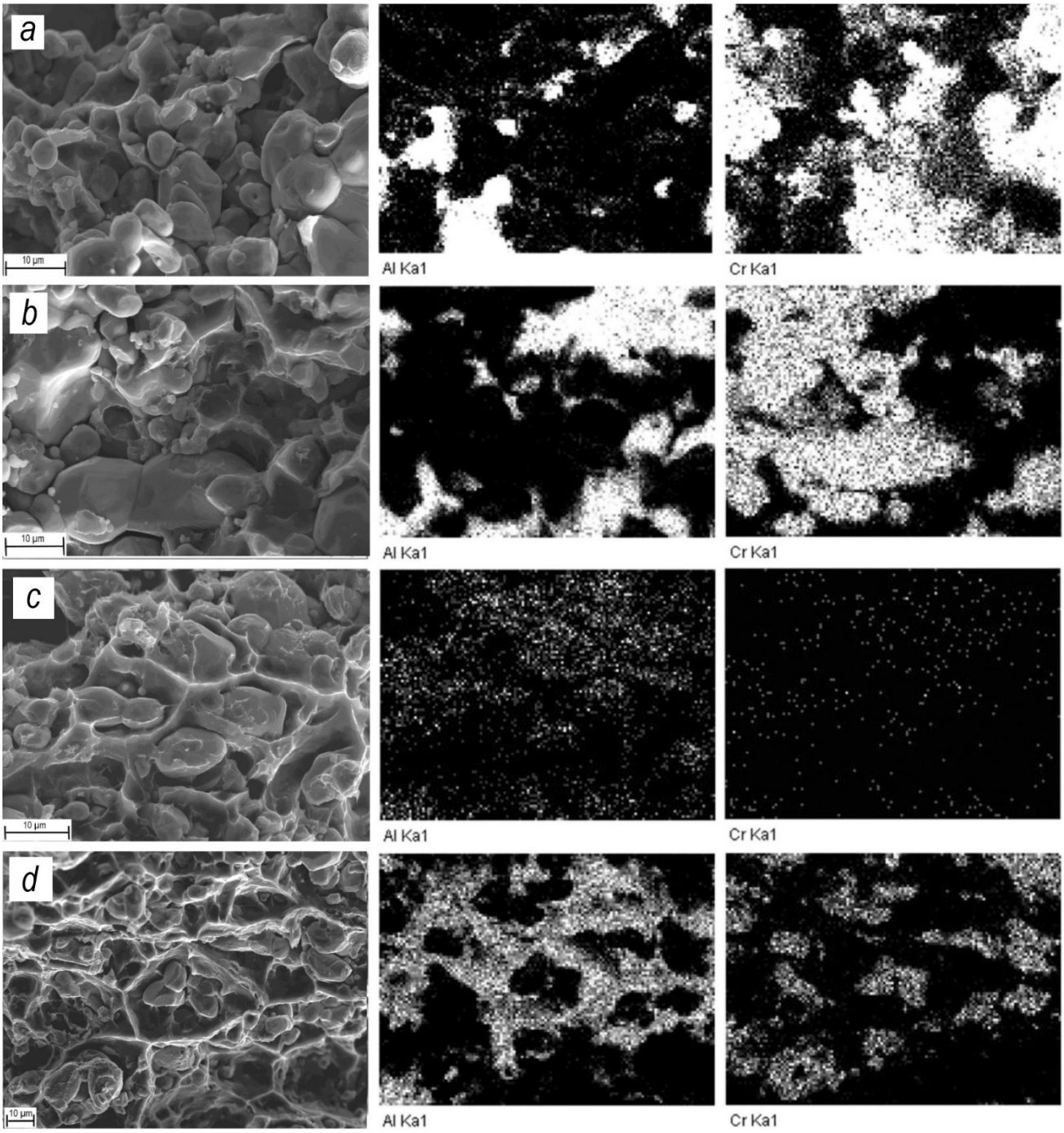

Figure 8. SEM image with element analysis of fracture surfaces of $Al_{70}Cr_{30}$ composites obtained under different conditions of hot compaction: (**a**) T= 350 °C, ε_n = 9%; (**b**) T= 550 °C, ε_n = 9%; (**c**) T= 350 °C, ε_n = 75%; (**d**) T= 550 °C, ε_n = 75%.

The evolution of the $Al_{65}Cr_{25}Si_{10}$ composite structure (Figure 9) with increasing temperature and deformation degree during hot compaction is not qualitatively different from the structure of the $Al_{70}Cr_{30}$ composite described above (Figure 8). Figure 9 shows the SEM image of the $Al_{65}Cr_{25}Si_{10}$ composite under minimum (Figure 9a) and maximum (Figure 9b) thermo-force impact. Arrow-pointed structure elements were identified by the EDX elemental analysis similar to that in Figure 8. At minimum temperature and deformation degree, the large aluminum particles are transformed in contact with harder particles of chromium and silicon, and the mutual deformation of adjacent particles of aluminum takes place. Fine particles of aluminum keep the shape close to the spherical

one (Figure 9a). The formation of continuous aluminum matrix in these conditions of thermomechanical processing does not occur, and there are no traces of ductile fracture. In these conditions, the strength of the composite does not exceed 20% of the maximum value, and the ductility is close to zero. When maximum temperature and maximum deformation are reached (T = 550 °C, ε = 75%), the continuous aluminum matrix with inclusions of chromium and silicon is formed (Figure 9b). On the fracture surface, the aluminum matrix ductile areas are combined with large particles of chromium and silicon protruded on rupture. The SEM image shows that the aluminum matrix under intensive thermomechanical processing flows into pore space and covers most of the chromium and silicon particles (Figure 9b).

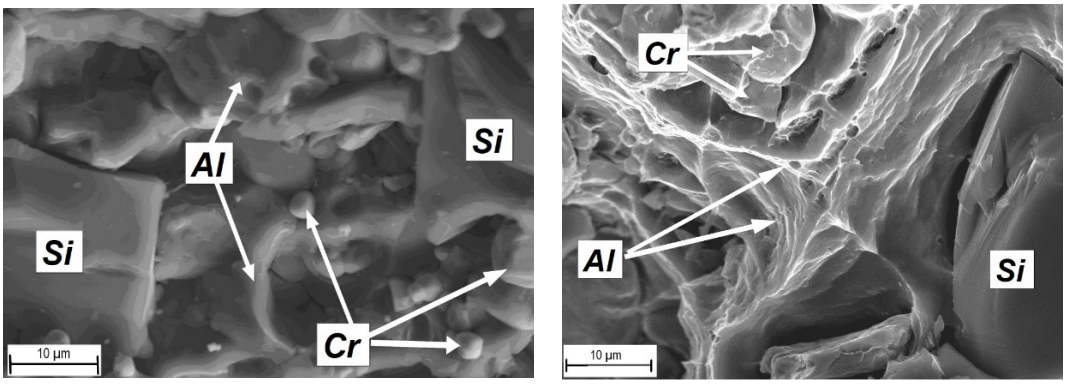

(**a**) (**b**)

Figure 9. SEM image of fracture surface of $Al_{65}Sr_{25}Si_{10}$ composite hot-compacted under ε = 9% at T = 350 °C (**a**) and ε = 75% at T = 550 °C (**b**).

The results of microstructure investigation and the comparison of physical–mechanical properties of the studied composites show that the strength, plasticity, and fracture behavior of composites are determined in general by structural states of the aluminum matrix. The strength and plasticity of the $Al_{65}Cr_{25}Si_{10}$ composite do not differ noticeably from the properties of the $Al_{70}Cr_{30}$ composite. It can be assumed that the addition of silicon in the composite does not lead to a significant deterioration of mechanical properties of composites with the decrease in aluminum matrix volume fraction.

4. Conclusions

The two-stage procedure for obtaining aluminum matrix composites enables us to produce powder material with low residual porosity. The preceding cold-pressing does not require high loads, since the subsequent stage of hot deformation can compact the green compact by up to 95–97% of density. The physical–mechanical properties and the fracture mode of the powder composites produced by hot deformation of the preforms cold-compacted from powder mixtures of aluminum, chromium, and silicon depend on the temperature and deformation degree during hot compaction.

The strength and ductility of composites are mainly determined by the aluminum matrix, which is formed by "welding" adjacent aluminum particles, and the presence of hard chromium particles does not impede this plastic flow of aluminum. The addition of silicon does not lead to noticeable change in mechanical properties of composites produced at high temperatures and high deformation degrees. Thus, the hot-compacted $Al_{70}Cr_{30}$ and $Al_{65}Cr_{25}Si_{10}$ powder composites can be used for medium-loaded parts and units, including cathode materials for vacuum arc deposition of wear-resistant coatings on tools.

Author Contributions: Conceptualization and experiment design, G.A.P. and V.V.K.; methodology, analysis, and discussion of results, manuscript writing, E.N.K. All authors have read and agreed to the published version of the manuscript.

Funding: This research was funded by government research assignment for ISPMS SB RAS, project FWRW-2021-0005.

Institutional Review Board Statement: Not applicable.

Informed Consent Statement: Not applicable.

Data Availability Statement: Data are contained within the article.

Conflicts of Interest: The authors declare no conflict of interest.

References

1. Vani, V.V.; Chak, S.K. The effect of process parameters in aluminium metal matrix composites with powder metallurgy. *Manuf. Rev.* **2018**, *5*, 1–13.
2. Rudianto, H.; Yang, S.S.; Kim, Y.J.; Nam, K.W. Sintering behavior of hypereutectic aluminum-silicon metal matrix composites powder. *Int. J. Mod. Phys. Conf. Ser.* **2012**, *6*, 628–633. [CrossRef]
3. Rajesh, A.; Santosh, D. Mechanical properties of Al-SiC metal matrix composites fabricated by stir casting route. *Res. Med. Eng. Sci.* **2017**, *2*, 1–6.
4. Tash, M.M.; Mahmoud, E.R.I. Development of in-situ Al-Si/CuAl2 metal matrix composites: Microstructure, hardness, and wear behavior. *Materials* **2016**, *9*, 442. [CrossRef]
5. Lavernia, E.J.; Ma, K.; Schoenung, J.M. Particulate reinforced aluminum alloy matrix composites—A review on the effect of microconstituents. *Rev. Adv. Mater. Sci.* **2017**, *48*, 91–104.
6. Moustafa, S.; Daoush, W.; Ibrahim, A.; Neubauer, E. Hot forging and hot pressing of AlSi powder compared to conventional powder metallurgy route. *Mater. Sci. Appl.* **2011**, *2*, 1127–1133. [CrossRef]
7. Popov, V.V.; Pismenny, A.; Larianovsky, N.; Lapteva, A.; Safranchik, D. Corrosion resistance of Al–CNT metal matrix composites. *Materials* **2021**, *14*, 3530. [CrossRef] [PubMed]
8. Šnajdar-Musa, M.; Schauperl, Z. ECAP—New consolidation method for production of aluminium matrix composites with ceramic reinforcement. *Process. Appl. Ceram.* **2013**, *7*, 63–68. [CrossRef]
9. Narayan, S.; Rajeshkannan, A. Studies on formability of sintered aluminum composites during hot deformation using strain hardening parameters. *J. Mater. Res. Technol.* **2017**, *6*, 101–107. [CrossRef]
10. Vojtěch, D.; Michalcová, A.; Novák, P. Structural evolution of Al-Cr alloy during processing. *Solid State Phenom.* **2008**, *138*, 145–152. [CrossRef]
11. Matvienko, O.; Daneyko, O.; Kovalevskaya, T.; Khrustalyov, A.; Zhukov, I.; Vorozhtsov, A. Investigation of stresses induced due to the mismatch of the coefficients of thermal expansion of the matrix and the strengthening particle in aluminum-based composites. *Metals* **2021**, *11*, 279. [CrossRef]
12. Rivera-Salinas, J.E.; Gregorio-Jáuregui, K.M.; Romero-Serrano, J.A.; Cruz-Ramírez, A.; Hernández-Hernández, E.; Miranda-Pérez, A.; Gutierréz-Pérez, V.H. Simulation on the Effect of Porosity in the Elastic Modulus of SiC Particle Reinforced Al Matrix Composites. *Metals* **2020**, *10*, 391. [CrossRef]
13. Chang, Y.-Y.; Chang, C.-P.; Wang, D.-Y.; Yang, S.-M.; Wu, W. High temperature oxidation resistance of CrAlSiN coatings synthesized by a cathodic arc deposition process. *J. Alloy. Compd.* **2008**, *461*, 336–341. [CrossRef]
14. Park, W.; Kang, D.S.; Moore, J.J.; Kwon, S.C.; Rha, J.J.; Kim, K.H. Microstructures, mechanical properties, and tribological behaviors of Cr-Al-N, Cr-Si-N, and Cr-Al-Si-N coatings by a hybrid coating system. *Surf. Coat. Technol.* **2007**, *201*, 5223–5227. [CrossRef]
15. Endrino, J.L.; Fox-Rabinovich, G.S.; Reiter, A.; Veldhuis, S.V.; Escobar Galindo, R.; Albella, J.M.; Marco, J.F. Oxidation tuning in AlCrN coatings. *Surf. Coat. Technol.* **2007**, *201*, 4505–4511. [CrossRef]
16. Polcar, T.; Cavaleiro, A. High-temperature tribological properties of CrAlN, CrAlSiN and AlCrSiN coatings. *Surf. Coat. Technol.* **2011**, *206*, 1244–1251. [CrossRef]
17. Kim, M.W.; Kim, K.H.; Kang, M.C.; Cho, S.H.; Ryu, K.T. Mechanical properties and cutting performance of CrAlN hybrid coated microtool for micro high-speed machining of flexible fine die. *Curr. Appl. Phys.* **2012**, *12*, 14–18. [CrossRef]
18. Sanchez, J.E.; Sanchez, O.M.; Ipaz, L.; Aperador, W.; Caicedo, J.C.; Amaya, C.; Hernandez Landaverde, M.A.; Espinoza Beltran, F.; Munoz-Saldana, J.; Zambrano, G. Mechanical, tribological, and electrochemical behavior of Cr1-xAlxN coatings deposited by reactive magnetron co-sputtering method. *Appl. Surf. Sci.* **2010**, *256*, 2380–2387. [CrossRef]
19. Pribytkov, G.A.; Korzhova, V.V.; Korosteleva, E.N. Solid-phase sintering of Al-Cr(Si, Ti) powder foundry alloys obtained by self-propagating high temperature synthesis. *Russ. J. Non-Ferr. Met.* **2013**, *54*, 252–260. [CrossRef]
20. Pribytkov, G.A.; Korzhova, V.V.; Savitskii, A.P. Structure, Strength and Fracture of Hot-Pressed Al-Cr, Al-Cr-Si Powder Composites. *AIP Conf. Proc.* **2014**, *1623*, 511–514.
21. Dorofeev, Y.G.; Bezborodov, E.N.; Sergeenko, S.N. Special features of formation of compacted material from mechanochemically activated fining of aluminum Alloy D16. *Met. Sci. Heat Treat.* **2003**, *45*, 73–75. [CrossRef]
22. Dorofeev, Y.G.; Bezborodov, E.N.; Sergeenko, S.N. Influence of kinetics of mechanochemical activation of aluminium powders on the processes of hot recompaction. *Phys. Chem. Mater. Treat.* **2002**, *4*, 79–81.

23. Sergeenko, S.N.; Alabid, N.S. Hot-deformed powder materials based on mechanochemically activated charges Al–SiC. *Tsvetnye Metally* **2016**, *9*, 1–6. [CrossRef]
24. Grushko, B.; Pavlyuchkov, D. Binary origin of the Al–Cr–Si τ_3-phase. *J. Alloy. Compd.* **2015**, *622*, 327–332. [CrossRef]
25. Zhou, Z.; Li, Z.; Wang, X.; Liu, Y.; Wu, Y.; Zhao, M.; Yin, F. 700 °C isothermal section of Al–Cr–Si ternary phase diagram. *Thermochim. Acta* **2014**, *577*, 59–65. [CrossRef]
26. Liua, X.; Beausir, B.; Zhang, Y.; Gand, W.; Yuan, H.; Yu, F.; Esling, C.; Zhao, X.; Zuo, L. Heat-treatment induced defect formation in α-Al matrix in Sr-modified eutectic Al–Si alloy. *J. Alloy. Compd.* **2017**, *9*, 1–27. [CrossRef]
27. Aqida, S.N.; Ghazali, M.I.; Hashim, J. Effects of porosity on mechanical properties of metal matrix composite: An overview. *J. Technol.* **2004**, *40*, 17–32. [CrossRef]
28. German, R.M. *Powder Metallurgy and Particulate Materials Processing*; Metal Powder Industries Federation: Princeton, NJ, USA, 2005; pp. 202–214.
29. Zhao, Q.; Yu, L.; Ma, Z.; Li, H.; Wang, Z.; Liu, Y. Hot Deformation Behavior and Microstructure Evolution of 14Cr ODS Steel. *Materials* **2018**, *11*, 1044. [CrossRef]